

Thermomechanical fatigue behavior of CGI 450 and CGI 500 cast irons

Márcio Henrique Ferreira¹

Douglas Giovanni Bon¹

Waldek Wladimir Bose Filho^{1*} 

Carlos de Souza Cabezas²

Wilson Luis Guesser (in Memoriam)^{2,3}

Abstract

The vermicular cast iron grade 450 is widely used in engineering applications, primarily by the automotive industry in the fabrication of internal combustion engines. However, in recent years, the vermicular cast iron grade 500 has been developed, and new studies searching for the replacement of the grade 450, with the aim of increasing the high-performance internal combustion engines life, as well as reducing their weight, are in development. Due to their operational characteristics, these engines are subjected simultaneously to thermal and mechanical cycles, which influence their useful life. Therefore, the characterization of the resistance to these types of loads for materials selection for these engines, is very important. Thus, the objective of this work was to study the thermomechanical fatigue life of two vermicular cast irons in conditions close to those to which internal combustion engines are subjected. The materials were characterized by chemical and metallographic analyses and tensile tests. The thermomechanical fatigue tests were carried out at temperatures ranging from 50 °C to 420 °C, and a dwell time of 180 seconds. The vermicular cast iron grade 500 exhibited higher tensile strength, with higher ductility when compared to the grade 450, as well as higher fatigue strength. These properties were related to the size and distribution of eutectic cells (graphite) in the matrix.

Keywords: Vermicular cast iron Class 450; Vermicular cast iron Class 500; Microstructure; Thermomechanical fatigue; Compacted graphite cast iron; Cylinder head.

Comportamento em fadiga termomecânica dos ferros fundidos vermiculares classe 450 e 500

Resumo

O ferro fundido vermicular da classe 450 é amplamente utilizado em aplicações de engenharia, principalmente pela indústria automobilística na fabricação de motores de combustão interna. Contudo, nos últimos anos, foi desenvolvido o ferro fundido vermicular da classe 500 e estudos têm buscado a substituição da classe 450, com o objetivo de aumentar a vida dos motores de combustão interna de alto desempenho, bem como a redução de seu peso. Devido as suas características operacionais, estes motores são simultaneamente submetidos a ciclos térmicos e mecânicos, que influenciam na vida útil destes e a caracterização da resistência a estes tipos de carregamentos para a seleção dos materiais para aplicação em motores, são muito importantes. Assim, o objetivo deste trabalho foi estudar a vida em fadiga termomecânica de dois ferros fundidos vermiculares em condições próximas das que os motores de combustão interna são submetidos. Os materiais foram caracterizados por meio de análise química, metalográfica e ensaios de tração. Os ensaios de fadiga termomecânica foram realizados em uma temperatura variando de 50 °C e 420 °C, e tempo de patamar de 180 segundos. O ferro fundido vermicular da classe 500 apresentou maior resistência mecânica em tração, com maior ductilidade comparado com o vermicular da classe 450, bem como maior resistência a fadiga. Estas propriedades estão relacionadas com o tamanho e distribuição das células eutéticas (grafita) na matriz.

Palavras-chave: Ferro fundido vermicular classe 450; Ferro fundido vermicular classe 500; Microestrutura; Fadiga termomecânica; Ferro fundido vermicular; Cabeçote de motor.

¹Escola de Engenharia de São Carlos, Universidade de São Paulo, USP, São Carlos, SP, Brasil.

²Tupy Foundry S.A, Joinville, SC, Brasil.

³Universidade de Santa Catarina, UDESC, Joinville, SC, Brasil.

*Corresponding author: waldek@sc.usp.br



1 Introduction

The CGI has the graphite cell in the vermicular form and this morphology offers a good combination of thermal and mechanical properties for component applications subjected to conditions of high temperature and pressure [1,2]. The shape, size and distribution of the graphite cells, as well as, the matrix phase composition, are the factors responsible for the resulting improved tensile strength when compared to gray cast iron [3]. According to Guesser [4], the graphite morphology is largely responsible for the mechanical strength level presented by the CGI cast irons [4,5]. Due to its low material and production costs (relative to Al cast alloys), and because its thermal and mechanical properties, make them suitable for applications to produce automotive components, such as the truck industry. An example is the cylinder heads of heavy-duty diesel engines, which are subjected to sudden temperature variations and pressure during the engine operation cycles. In this component, its complex geometry and thin sections in some parts, submit the material to large thermal gradients in very close regions, generated by the rapid heating at the ignition valves and, at the same time, cooled by the engine's cooling system, restricting the material's thermal expansion [1,4]. This mechanical restriction, introduce high local compressive stresses at high temperature, causing micro plastic deformations in regions where the yield limit has been reached [5]. After the engine is switched off, the temperature drops, and high tensile stresses are developed, because of the previous plastic deformations in compression. These internal stresses, generated by the combustion engine regular in-service cycles (starting, operating, and shutting down), reveal a stress-strain hysteresis cycle, called out-of-phase thermomechanical fatigue (OP-TMF) [6]. Consequently, cracks may nucleate and growth between the valves bridges, as can be seen in Figure 1, which can lead the component to complete failure. Seeking to reduce carbon emissions into the atmosphere and at the same time, improve the heavy-duty engine performance, the truck industry has been pushed to find the solutions by developing new projects and the use of more resistant materials, so that the engine efficiency can be achieved without compromising durability, nor explicitly increasing production costs [7,8]. The main objective of this work is to study the behavior of thermomechanical fatigue in two cast irons, a compact one of class 450 and a vermicular one of class 500, through tests that simulate the real conditions of temperature and load, during the period of operation of the engine. internal combustion diesel. Thus, the CGI500 showed better results in mechanical strength and fatigue compared to the CGI450.

2 Materials and methods

The materials analyzed in this work are two compacted cast irons, named CGI 450 and CGI 500. Both materials were taken directly from cylinder heads, produced according to alloying specification and processing recommended by the Brazilian foundry industry TUPY S.A. - Joinville SC, Brazil. Table 1 presents the nominal chemical composition for both classes CGI450 and CGI500, since the actual materials chemical composition and processing details are not provided due to industrial confidentiality.

2.1 Metallographic analysis

The microstructural analysis was performed using a ZEISS model LAB microscope. A1 equipped with AXIO brand camera model ERC5s, software AXIO VISION Rel.4.8, to obtain images with magnifications of 50, 100, 500 and 1000x, in order to analyze the size and morphology of graphite, quantify its percentage, as well as the matrix constituents.

2.2 Tensile test

The tensile tests were carried out at ambient and high temperatures, according to ASTM E8M [9] and ASTM E21 [10] standards. The test temperatures were 50 °C and 420 °C with a cross head speed of $1.6 \times 10^{-2} \text{ mm.s}^{-1}$, being obtained the values of the elastic modulus, E, yield limit, Sy, ultimate tensile



Figure 1. Failed cylinder head due to TMF process. It is observed a crack (arrow) at the valves bridge. Picture taken in a Brazilian automotive workshop.

Table 1. Nominal chemical composition.

Class	Chemical Elements					Mo
	C	Si	Mn	Cu	P	
CGI 450	3.5 – 3.8	2.1 – 2.6	0.3 – 0.5	0.6 – 1.0	< 0.065	-
CGI 500						0.1 – 0.35

stress, S_{UTS} , and total elongation. For testing it was used a MTS close loop servo hydraulic dynamic system, model 810, with a maximum load capacity of 250 kN. Figure 2 shows the geometry and dimensions of the specimen prepared according to the ASTM E8M [9] technical standard.

2.3 Thermomechanical fatigue

The thermomechanical fatigue tests were designed to be as close as possible to the in-service conditions of the cylinder heads of heavy-duty combustion engines, more precisely to reproduce the thermomechanical conditions of the valves bridge regions from specimens similar to Figure 1.

Therefore, tests were carried out in strain control, under 100% mechanical constraint, tensile stress out-of-phase with the maximum temperature, this is, the highest tensile stress occurs at the lowest thermal cycle temperature. The OP-TMF test temperatures varied between 50 °C and 420 °C, with a 180 s dwell time at 420 °C. The system for the thermal cycle test consists of an inductive oven connected to a programmable temperature controller. A 5 mm diameter copper coil, cooled with running water, was used to heat the specimens and an air blowing system was used during the cooling part of the thermal cycles. For strain control an extensometer with ceramic rods were used.

3 Results

Figure 3a presents the general view of the CGI 450 cast iron without etching, and the results showed that the microstructure

presents 10% of graphite cells. After etching with 2% Nital, Figure 3b, it is observed that the matrix is composed by 93% of pearlite and 7% of ferrite. The graphite was classified according to the SAE J1887 [11] standard as type III-VI containing 10% nodularity. The black features are graphite phase and the white regions around the arms is ferrite, and the rest is pearlite.

The CGI 500 shows a quite similar microstructure, see Figure 4a, with 9.6% of type III-IV graphite particles with 24% nodularity. It is observed also, that the graphite cells are smaller and less connected (CGI 450 = 433 μ m and CGI500 = 337 μ m [12]). The matrix, Figure 4b, are mainly composed of pearlite.

The tensile parameters obtained for both materials are in accordance with their respective grades and presented in Table 2. According to the SAE J1887 [11] standard, increased mechanical strength is expected for CGI 500, since it presents larger alloying solid solution strengthening, pearlite refining (Mo addition), as well as, the graphite cells size (more refined) and morphology (in CGI 450, they are more needle like ends, while in the CGI500 the worms present quite rounded ends, see Figures 5a and b). Another important factor is the higher nodularity in the CGI 500.

The temperature variation during the thermal cycle, in the range of 50° to 420 °C ($\Delta T = 320$), leads to a thermal strain of 0.58% ($\alpha = 15.6 \times 10^{-6}$). Figure 6a shows the stress and temperature variation with time of the OP-TMF tests.

Both compacted cast irons exhibited quite similar stress-strain behavior, as shown in Figure 6b and Table 3. Thus, during the heating step a very high compressive stresses are generated at the first cycle that is quite important in determining the thermomechanical fatigue life.

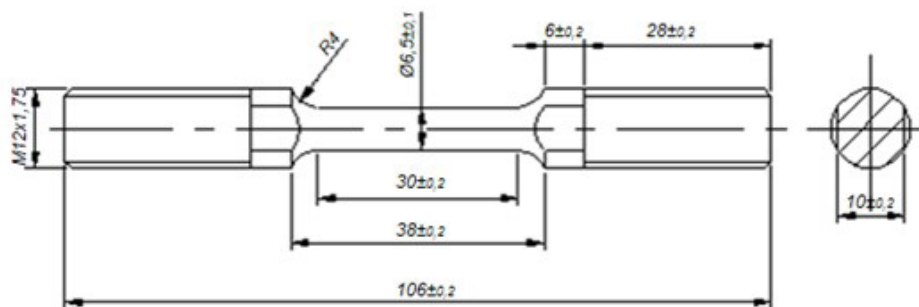


Figure 2. Geometry and dimensions of the specimen used in the tensile test.

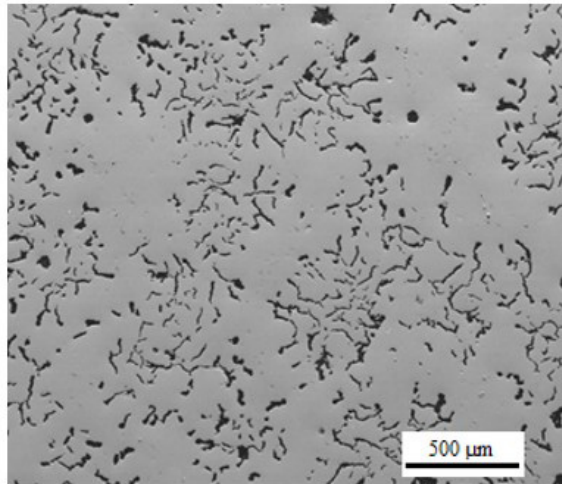
Table 2. Tensile test results for cast irons classes CGI-450 and CGI-500

Material	Temp. °C	S_{UTS} , MPa	S_y , MPa	E, GPa	El, %	
CGI-450	50	493[15]	344[13]	150[17]	2.5[1]	SD []
	420	411[23]	282[19]	119[21]	3.0[1]	
CGI-500	50	566[21]	361[25]	147[20]	3.5[1]	
	420	448[28]	298[29]	133[27]	3.4[1]	

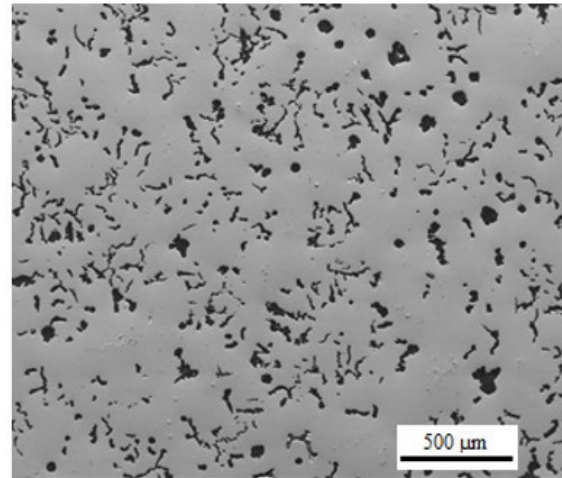
SD: standard deviation. Números entre colchetes se referem ao valores do desvio-padrão.

In this cycle, as the temperature gradually increases to 420 °C, the total deformation remains constant and close to zero (100% constraint), as the thermal deformation builds up, it is counterbalanced by an equivalent mechanical deformation in the opposite direction, creating a compressive stress as shown in Figure 6a. The generated stresses are sufficient to cause yielding, first in compression and lately in tensile, as shown by Figure 6b, causing plastic deformation

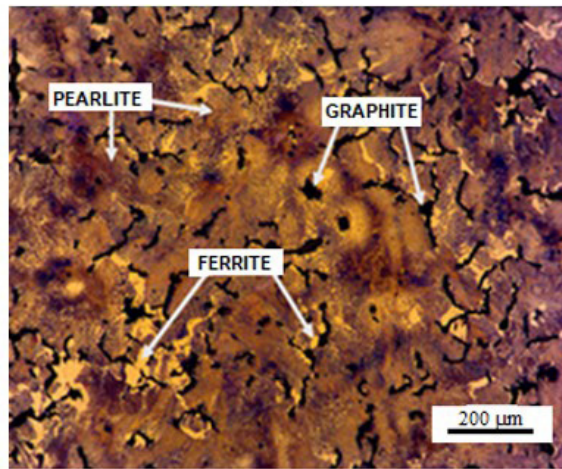
in both cases. Also, it is observed stress relaxation due to the yielding at the cycle plateau of 180 seconds at 420 °C, with the stress dropping from approximately 370 to 250 MPa. At this point, the cooling part of the thermomechanical cycle starts, leading the compressive stress to zero and lately to tensile stress (developed due to the plastic deformation from the first heating cycle), followed by a quite small stress relaxation.



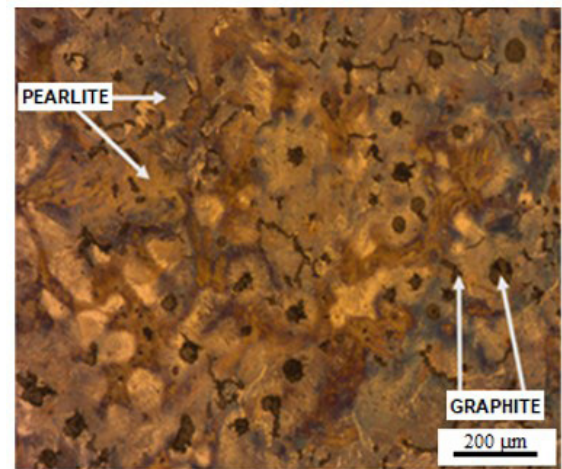
(a)



(a)



(b)



(b)

Figure 3. CGI 450 (a) SEM micrograph showing the distribution of graphite cells and (b) OM of matrix etched with 2% Nital.

Figure 4. CGI 500 (a) SEM micrograph showing the distribution of graphite cells in the CGI-450, (b) OM of the matrix etched with 2% Nital.

Table 3. Thermomechanical fatigue test results, cycles to failure and maximum stress, S_{max}

Material	SP (Specimen)	N_f	Average	S_{max} *	Average	SD
CGI-450	1	275	289[49]	356	355[15]	SD []
	2	349		350		
	3	233		364		
	4	296		353		
CGI-500	1	582	649[124]	365	358[28]	
	2	680		351		
	3	527		367		
	4	810		350		

SD: standard deviation. Números entre colchetes se referem ao valores do desvio-padrão.

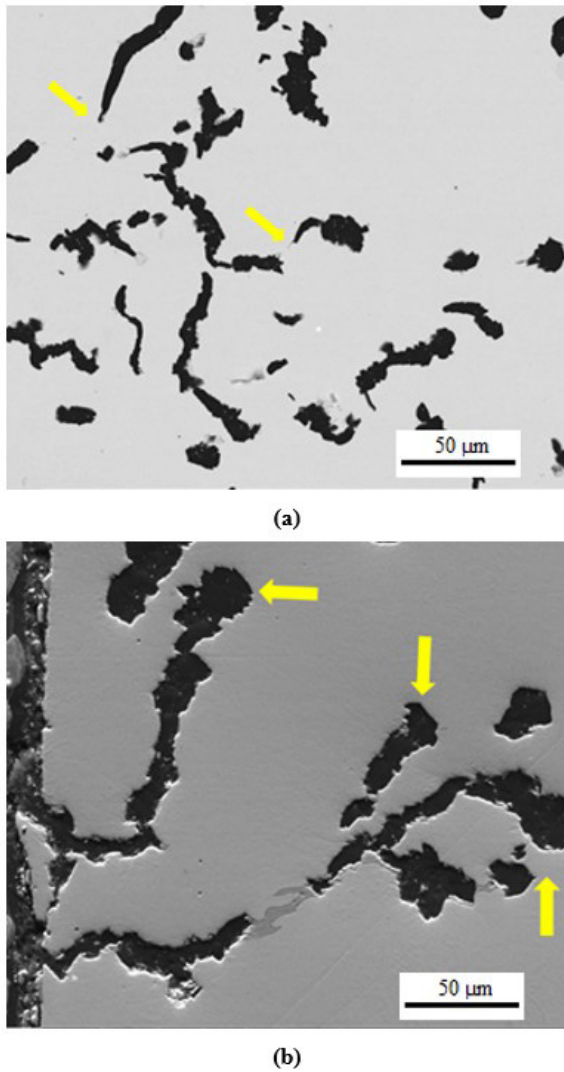


Figure 5. Graphite worms with rounded tip for (a) CGI 450 and (b) CGI 500.

From the OP-TMF results in Table 3, it is clear the superior CGI 500 fatigue resistance, it exhibiting 125% longer life than the CGI450.

The fracture surface SEM analyses showed strong evidences that, soon the OP-FTM test starts, cracks occur between the matrix/graphite interfaces (Figure 7) as reported previously by Norman et al. [13].

As shown in Figure 8 and Figure 9a for the CGI 500, cracks start from graphite particles at or close to the specimen surface, with crack growth through the pearlitic matrix by fatigue striation (Figure 9b) with a cleavage appearance (grey phase), and by graphite matrix interface (black phase), until final failure by mixture of ductile and cleavage modes [12,14,15]. The cavities or rounded features observed on the fracture surface are voids left by the graphite or from the graphite that stayed in the other half [14,16].

As observed, soon the OP-FTM test starts, cracks initiate at the graphite cells interfaces with the matrix, with

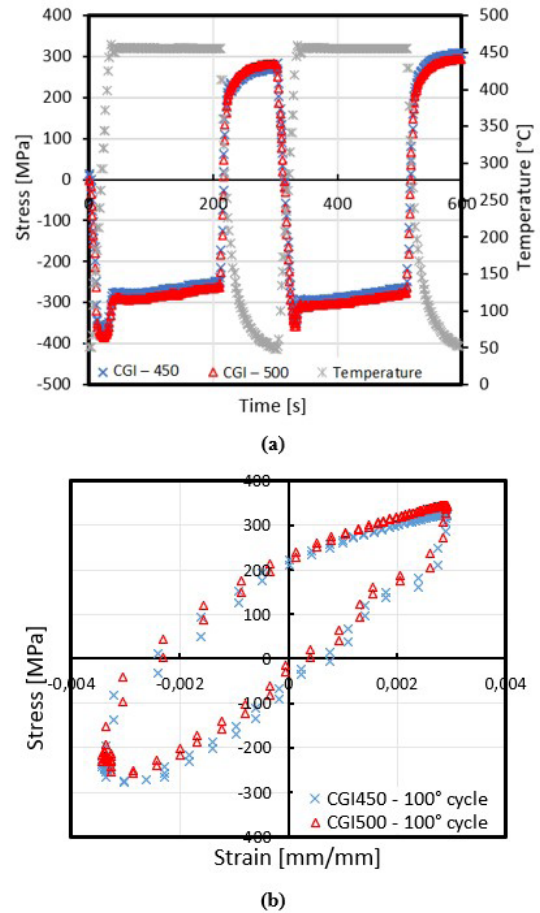


Figure 6. Hysteresis obtained in 100th cycle by FTM of CGI 450 and CGI 500.

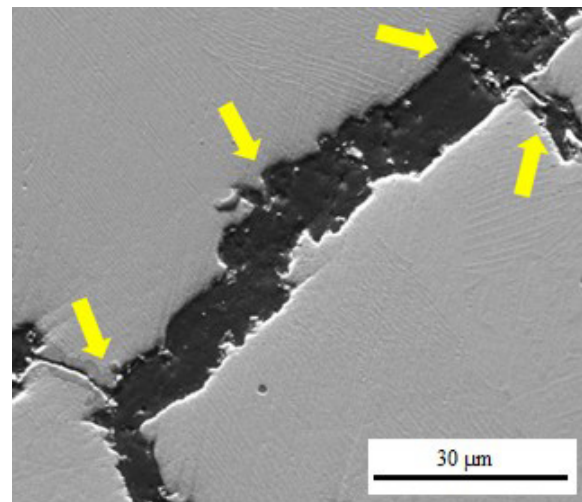


Figure 7. The crack propagated preferably through the graphite/matrix interface. CGI 500, 380 cycles.

the graphite cell boundaries and dendrites representing a barrier for newer crack extension, as shown in Figure 7, between the yellow bars.

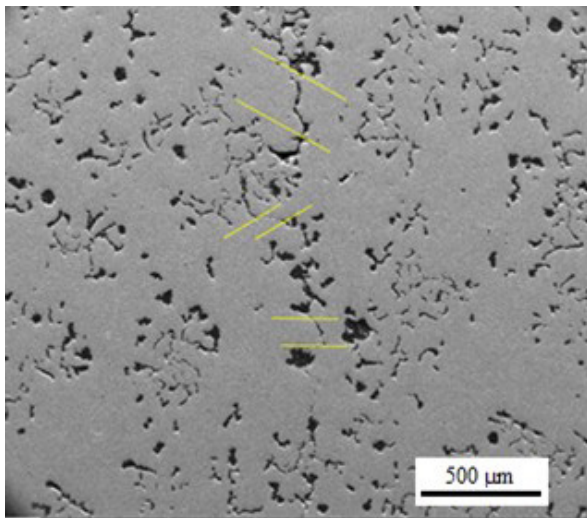


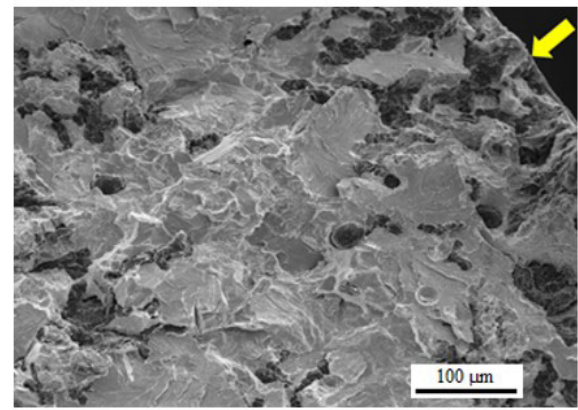
Figure 8. From one eutectic cell to another, the crack had to go through the matrix (eutectic cell boundary or dendrite).

The great difference between the CGI 450 and 500 cast irons are the matrix microstructural characteristics (refined pearlitic matrix without ferrite), size and distribution of the graphite cells (smaller graphite cells with larger matrix spacing between them), and primary, the shape of the graphite worms ending (graphite worms with rounded ends). The contributions of all these features lead to an enhancement of the OP-TMF resistance

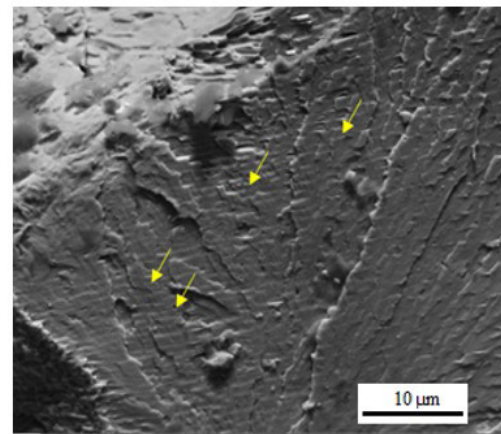
It is important to observe that oxidation process at the crack tip, takes part in the crack growth process, however, by simplicity of analyses it was not discussed here. This effect on the OP-TMF processes should be discussed in further research work.

4 Discussion

Through the results from this work and also from other authors [12,15,16], it was concluded that the connectivity of graphite cells, their size and distribution, directly affects the compacted cast iron properties, such as mechanical strength, fatigue and thermal conductivity. As the graphite cells are crucial for the cast iron properties, the results obtained for the CGI500 showed an enhanced mechanical strength and OP-TMF resistance in relation to the CGI450. These results are in accordance to the ones obtained by other researchers under similar conditions [5,15]. The main differences between CGI450 and CGI500 are related to a more refined pearlitic structure and size and distribution of the eutectic cells, these features lead to a stronger matrix and lower eutectic cells connectivity. From the interrupted tests, it was observed the existence of non-propagated very small cracks in both cast irons, but the CGI500 longer life was mainly due to the larger spacing among the eutectic cells [16,17]. Table 4 shows the morphologic characteristics for CGI 450 and CGI 500 compacted cast irons. Thus, the better resistance



(a)



(b)

Figure 9. CGI 500. (a) Fracture surface showing the initiation site and (b) the fatigue crack growth by plastic deformation (fatigue striations) in a "cleavage like" fracture surface.

Table 4. Average size of the eutectic cells of compacted cast iron class 450 and class 500

	CGI 500	CGI 450
Cell size (μm)	395	433
Average graphite particle size (μm)	33	40
Graphite particle /mm ²	251	242

of the CGI-500 to crack propagation is due to the frequent decelerations due to its graphite shape (more rounded ends), better distribution and interconnectivity, forcing the crack to travel through the matrix region, requiring greater energy expenditure, consequently delaying its growth [18,19].

5 Conclusions

In this work the following conclusions are made:

- CGI 450 and CG500 cast irons have a microstructure composed of vermicular graphite cells in a pearlitic

matrix. The CGI450 presents a small amount of ferrite, while the CGI 500 exhibits a more refined pearlitic structure with twice amount of nodular graphite;

- As expected, the CGI 500 presents slightly higher mechanical strength and ductility than the CGI450;
- The OP-TMF results showed that the CGI 500 has an amazing fatigue resistance, exhibiting 125% longer life than the CGI450. This enhanced TMF resistance is due to different microstructural features, such as:

refined pearlitic matrix without ferrite, smaller mean graphite cells with larger matrix spacing among cells and the shape of the graphite worms with more rounded ends.

Acknowledgements

The Authors would like to thank TUPY for the financial support and for providing the materials and SMM-USP for providing the research facilities.

References

1. Trampert S, Gomez T, Pischinger S. Thermomechanical fatigue life prediction of cylinder heads in combustion engines. *Journal of Engineering for Gas Turbines and Power*. 2008;130(1):012806.
2. Guesser WL, Guedes LC. The new generation of engines and the challenges for the foundry industry. São Paulo: AEA SIMEA, Brasil; 2016 [cited 2021 Oct 20]. Available at: <http://pdf.blucher.com.br.s3-sa-east-1.amazonaws.com/engineeringproceedings/simea2016/PAP14.pdf>
3. Langmayr F, Zieher F, Lampic M. The thermo-mechanics of cast iron for cylinder heads. *MTZ Worldwide*. 2004;65:17-20.
4. Guesser WL. *Propriedades mecânicas dos ferros fundidos*. São Paulo: Editora Blucher; 2019.
5. Tillmann CADC. *Motores de combustão interna e seus sistemas*. Pelotas: Instituto Federal de Educação, Ciência e Tecnologia. 2013. p. 9-25.
6. Löhe D, Tillmann B, Lang KH. Important aspects of cyclic deformation, damage and lifetime behavior in thermomechanical fatigue of engineering alloys. In *Proceedings of the 5th International Conference on Low Cycle Fatigue*; 2003; Berlin. Vienna, Austria: IAEA; 2003. p. 161-176.
7. Norman V. *Fatigue of heavy-vehicle engine materials: experimental analysis and life estimation [thesis]*. Linköping University Electronic Press; 2018.
8. Bignonnet A, Charkaluk E. Thermomechanical fatigue in the automotive industry. *European Structural Integrity Society*. 2002:319-330.
9. ASTM International. *ASTM E8/E8M: Standard test methods for tension of metallic materials*. West Conshohocken, PA: ASTM; 2014.
10. ASTM International. *ASTM E21: Standard Test Methods for Elevated Temperature Tension Tests of Metallic Materials*. West Conshohocken, PA: ASTM; 2017.
11. SAE International. *SAE J1887/2002: Automotive Compacted Graphite Iron Castings*. Pensilvânia, EUA: SAE International; 2007.
12. Bon DG, Ferreira MH, Bose WW Fo, Guesser WL. Fracture micromechanisms evaluation of high-strength cast irons under thermomechanical fatigue conditions. *International Journal of Metalcasting*. 2020;14(3):696-705.
13. Norman V, Skoglund P, Moverare J. Damage evolution in compacted graphite iron during thermomechanical fatigue testing. *International Journal of Cast Metals Research*. 2016;29:1-2, 26-33.
14. Bon DG. *Vida em fadiga isotérmica e termomecânica de ferros fundidos cinzento classe 300 e vermicular classe 500 [dissertation]*. São Carlos: Universidade de São Paulo; 2020.
15. Ghodrat S. *Thermo-mechanical fatigue of compacted graphite iron in diesel engine components [thesis]*. Delft University of Technology; 2013.
16. Ghodrat S, Riemslog TAC, Kestens LAI, Petrov RH, Janssen M, Sietsma J. Effects of holding time on thermomechanical fatigue properties of compacted graphite iron through tests with notched specimens. *Metallurgical and Materials Transactions A*. 2013;44:2121-2130.
17. Ferreira MH. *Análise da vida em fadiga termomecânica de ferros fundidos cinzento e vermicular [dissertation]*. São Carlos: Universidade de São Paulo; 2017.
18. Skoglund P, Elfsberg J, Ipek N, Diaconu LV, Larsson M, Schmidt P. Thermo-mechanical fatigue of grey cast iron for cylinder heads-effect of niobium, molybdenum and solidification time. *Materials Science Forum* 925:377-384.

- 19 Ott SM. Efeito do molibdênio no comportamento em fadiga térmica de ferros fundidos vermiculares [dissertation]. Porto Alegre: Universidade Federal do Rio Grande do Sul; 1999.

Received: 13 Sep. 2021

Accepted: 17 Aug. 2022